Int. J. Heat Mass Transfer. Vol. 22, pp. 267–277

0017-9310/79/0201-0267 $02.00/0

THE DEVELOPMENT OF TURBULENT TRANSPORT IN A VERTICAL NATURAL CONVECTION BOUNDARY LAYER

R. G. BILL, JR.* and B. GEBHART†

(*Received* 14 *February* 1978 *and in revised form* 10 *May* 1978)

Abstract—Three calibrated hot-wire sensors and a thermocouple were used to measure the longitudinal and normal components of velocity, u and v, and the temperature, t, in the transition flow regime of the buoyancy induced boundary layer adjacent to a constant heat flux vertical surface. Analog signals of the sensor were digitized and recorded on magnetic tape in real time. The digital data were processed using a fast–Fourier transform algorithm to calculate variances, $\overline{u'^2}$, $\overline{t'^2}$; covariances, $\overline{u'v'}$, $\overline{v't'}$, correlation coefficients, $R_{v't'}$, $R_{u't'}$; and variance spectra of $\overline{u'^2}$ and $\overline{t'^2}$. In transition, velocity and temperature fluctuation levels, $\overline{u'^2}$ and $\overline{t'^2}$, increased with increasing distance downstream and the disturbance spectrum broadened to a larger range of frequencies. At the end of transition, the growth of velocity fluctuations, $\overline{u'^2}$, was sharply reduced. However, another flow regime beyond transition was identified in which the spectra of velocity fluctuations continued to broaden and temperature fluctuation levels $\overline{t'^2}$, as well as turbulent heat fluxes continued to increase.

NOMENCLATURE

- C_p, specific heat of fluid;
- g, gravitational acceleration;
- G, stability Grashof number based on heat flux, $5 \cdot (g\beta x^4 q''/5k2^2)^{1/5}$;
- h, heat-transfer coefficient;
- k, thermal conductivity of fluid;
- q'', local plate heat flux;
- $R_{\alpha'\beta'}$, correlation coefficient between variables α' and β';
- t', instantaneous temperature fluctuation;
- u', instantaneous x velocity component fluctuation;
- v', instantaneous y velocity component fluctuation;
- x, vertical distance along heated surface;
- y, normal distance from heated surface.

Greek symbols

- β, volumetric temperature coefficient of fluid;
- $\phi_{\alpha'\beta'}$, spectral or cospectral density of variable $\alpha'\beta'$;
- ν, kinematic viscosity of the fluid.

Superscript

- $\overline{\ }$, time averaged quantities.

1. INTRODUCTION

EXTENSIVE research of natural convection boundary layers has delineated many of the steps in the transformation of laminar to turbulent flow. These advances in understanding have been achieved primarily through the measurement of mean velocity and temperature profiles, without recourse to detailed statistical measurements. In order to complete the picture of transition however, an increased knowledge of energy spectra and of turbulent heat and momentum flux is necessary. Such measurements can illuminate and extend understanding gained from past studies.

Gebhart [1] has reviewed the early stages of transition in which instability is dominated by random two-dimensional disturbances of sinusoidal form. Data for external natural convection flows indicate the complete success of linear stability theory in predicting both the frequency and growth rate of disturbances in the early stages of instability.

Natural transition on a vertical constant heat flux plate in water was investigated by Jaluria and Gebhart [2] using primarily a single hot-wire probe and thermocouple. Prior to the beginning of transition, disturbances were characterized by a single frequency, in agreement with the linear stability filtering mechanism. However, as the end of transition was approached, an inspection of analog records of the anemometer and thermocouple outputs indicated the progressive increase in disturbance frequency. Surprisingly, disturbances with frequencies predicted by the filtering mechanism were still observed, even to the end of transition.

Distributions of disturbance levels in the boundary layer showed local maxima occurring at two locations across the boundary layer. The growth of the periodic disturbance maxima, with distance along the plate, initially increased according to the prediction of linear stability theory. The growth rate then finally decreased until the magnitude was less than the linear theory prediction.

The measurements of Jaluria and Gebhart [2]

*Assistant Research Scientist, Office of Water Resources and Dept. of Fruit Crops, University of Florida, Gainesville, FL, U.S.A.

†Dept. of Mechanical Engineering, SUNY at Buffalo, Buffalo, NY, U.S.A.

confirmed the existence of a Prandtl number, Pr, dependent transition mechanism, first observed by Godaux and Gebhart [3]. Godaux and Gebhart [3] investigated transition on a constant flux, vertical plate in water, $Pr = 6.7$, using thermocouples and a single hot wire. They observed that transition, occurring first in the thicker velocity boundary layer, triggered the beginning of transition in the thermal boundary layer, along with the increase in local heat transfer rate associated with transition.

Jaluria and Gebhart [2] further confirmed the observation of Godaux and Gebhart [3] that transition was a function not only of the local Grashof number, as would be expected from linear stability theory, but a function of the plate heat flux, q'', or equivalently, the longitudinal coordinate, x. Detailed velocity and temperature measurements indicate that velocity transition (as indicated by a jump in the frequency of disturbances above that resulting from the filtering mechanism) was a function of the kinetic energy flux. This parameter was found to correlate reasonably well with data available involving fluids with a wide range of Prandtl number. Furthermore, the correlation apparently accommodates a change in boundary condition from constant flux to isothermal.

Few other experimental studies have been made of the mechanism of actual transition in natural convection. Some experimental data exist, but most of them are in the form of heat-transfer rates and mean temperature profiles. An extensive review of such studies of transition for vertical natural convection boundary layers is given by Jaluria and Gebhart [2].

In the fully developed turbulent regime, considerable statistical information has now been gathered on vertical natural convection flows, Kutateladze *et al.* [4] determined profile of the mean velocity, u, and turbulent fluctuations, $\overline{u'^2}$ on an isothermal plate in ethyl alcohol using the method of stroboscopic flow visualization, with particles of aluminum in the fluid. Profiles of the turbulent fluctuations $\overline{u'^2}$ indicated a sharp peak occurring at the location of the maximum of the profile of mean longitudinal velocity.

Papailou and Lykoudis [5] measured mean temperatures, with iron–constantan thermocouples, and temperature fluctuation levels, $\overline{t'^2}$, with hot-film probes in mercury, in the turbulent boundary layer formed along the isothermal wall of a cell. Measurements of the temperature fluctuations in the longitudinal direction along the plate, indicated that the intensity of fluctuations first increased then decreased. A profile of turbulent temperature fluctuations, $\overline{t'^2}$, across the flow region, indicated a fairly broad maximum near the wall. The spectral densities of the temperature fluctuations were measured using an electronic spectrum analyzer. The spectra at the outer portion of the boundary layer indicated a slight convective subrange, that is, the "$-5/3$" spectrum predicted by Corrsin [6]. Spectra calculated near the wall, however, completely lacked a convective subrange or contained one which extended over a very small range of wave numbers. A substantial "-3" range is observable in all the spectra. This range corresponds to the buoyancy range predicted by Shur [7] and Lumley [8], in which the cascade of energy in the inertial range is affected by the production of turbulence due to buoyancy forces.

The most extensive measurements to date in a turbulent natural convection boundary layer have been those of Smith [9] on an isothermal plate in air. Profiles of mean longitudinal velocity, u, and normal velocity, v, are presented along with mean temperature, t, profiles. Profiles of turbulent fluctuations, $\overline{u'^2}$, $\overline{v'^2}$, and $\overline{t'^2}$ are present along with covariances $\overline{u't'}$, $\overline{v't'}$, and $\overline{u'v'}$ and the associated correlation coefficients and spectra and cospectra.

A comparison of the transition results of Jaluria and Gebhart [2] and the heat-transfer results of Vliet and Liu [10] for the constant flux plate in water indicates that an additional transition stage must occur beyond that reported by Jaluria and Gebhart [2]. At the end of transition, both the thermal and velocity intermittency factors (the fraction of the time the flow is not laminar) are one except at the outer edge of the boundary layer where intermittency must fall to zero. However, the data of Vliet and Liu [10] indicates that beyond the end of transition the local heat-transfer coefficient, h, continues to rise sharply despite the total disappearance of the laminar flow regime. Eventually, further downstream, the growth of the local heat-transfer coefficient comes to a halt. Then the coefficient, h, decreases with distance downstream at a rate similar to the decrease in the laminar boundary layer.

The spectral results of this investigation indicate that the initial sharp increase in heat transfer reported by Vliet and Liu [10], as well as the disruption of the laminar flow reported by Jaluria and Gebhart [2] occur while disturbances are characterized primarily by large scale eddies. Although non-linear processes, as observed by Jaluria and Gebhart [2], have already led to complicated flow patterns, most of the disturbance energy is distributed at or below the filtered frequency predicted by linear stability theory. Non-linear processes then continue and feed energy to disturbances of higher frequency. Thus the flow regime beyond the end of transition may be termed the regime of spectral development. The upper broadening of the spectrum must eventually be terminated at an upper frequency associated with the smallest eddy sizes at which turbulence is dissipated by molecular viscosity.

A parallel explanation for the delay in the occurrence of developed turbulence, beyond the end of transition, is the continued lag in the development of temperature disturbance levels observed in transition by Jaluria and Gebhart [2]. In this study,

temperature disturbance levels were observed to rise sharply beyond the end of transition despite the levelling of the growth of velocity disturbances. The decrease of the growth rate of temperature disturbance levels, like the end of spectral development, corresponded well with the beginning of developed turbulence, is indicated by the heat-transfer data of Vliet and Liu [10].

2. THE EXPERIMENT

The experiment followed closely the methods of Jaluria and Gebhart [2] and of Godaux and Gebhart [3]. The flow was generated adjacent to a uniform flux, flat, vertical surface. The surface was a 132 cm high and 41.5 cm wide Inconnel 600 foil assembly, which consisted of two foils 0.00127 cm thick bonded together by layers of Teflon. The assembly was bonded at high pressure and temperature to fuse the Teflon to the foil. The final thickness of the assembly was 0.038 cm.

The foil assembly was then stretched vertically between two knife edges. The foil was heated electrically by means of three Nobatron MR36-30 DC power supplies, placed in parallel. The heat flux through the assembly was inferred from the measurement of the voltage drop across the foil and the current flowing through a shunt resistor in series with the foil. As the flux is obtained from electrical dissipation, the conditions of uniform surface flux is achieved for a foil of uniform thickness.

The investigation was carried out in a $2 \times 1\text{–}2/3 \times 3$ m high insulated tank made of stainless steel with glass windows. The leading edge of the foil was 15 cm from the bottom of the tank and the trailing edge was 25 cm from the water–air interface. Resistivity of the water in the tank was increased to approximately 1.2 MΩ cm using a water purification system described in detail by Hollasch [11]. Over a period of approximately one month, the purity of the water degraded due to the sensitivity of pure water to contact with carbon dioxide in the air. The results reported here were achieved under conditions for which the resistivity was greater than 0.8 MΩ cm. Water of this purity was needed to avoid "drift" in the use of bare hot wires. Only stainless steel, Teflon and glass were allowed to come in contact with the water except where electrical connections made the use of silicone seal, as an insulator, necessary.

The thermal capacity of foil assembly was sufficiently small so that steady state was achieved within a few minutes (1–2 min depending upon the foil heat flux). The large size of the tank made a long test time 20–25 min possible without causing stratification or circulation in the tank. The total temperature difference across the boundary region was usually of the order of 2–5°C.

The three components of velocity, and the temperature, were determined using a probe consisting of 3 hot wires and a 76 μm copper–constantan thermocouple referenced to an ice bath junction. Two hot-wires (DISA probe 55A36) in an "inverted V" were placed parallel to the vertical surface. A third hot-wire (DISA probe 55A29) was positioned less than 1 mm from the apex of the "V" so as to be normal to the foil surface. The hot-wire sensors were made of 12.7 μm dia platinum. Connectors to the probe were standard DISA equipment and voltage outputs were obtained from DISA 55D01 anemometer units. The hot-wire overheat ratio was 1.1. This resulted in a sensor temperature of about 34°C above the ambient. The thermocouple was placed adjacent to the hot-wire, approximately 2 mm from the bottom of the "V".

Calibration of the hot-wires was achieved in water of resistivity of about 1 MΩ cm by the method of Hollasch and Gebhart [12]. The probe configuration during calibration was the same as that used in the experiment. The hot-wire sensors were calibrated over a velocity range of 0.06–3.3 cm/s in ambient water. The probe calibration was tested by measuring the laminar velocity base flow, for a heat flux of 95.3 W/m^2 and at a downstream location of 48.3 cm. The deviation from laminar theory was maximum at the velocity peak, being high by 6%. Beyond the inflexion point the measured velocity was low by less than 5%. It should be noted that the use of a temperature correction such as that of Hollasch and Gebhart [12], which would take into account the temperature gradient in the boundary layer, would lead to a greater deviation from laminar theory. As no known previous experiments in natural convection using similar probes were available for guidance in matters of length or temperature corrections, and since all measurements were taken beyond the region of high temperature gradient no corrections were employed.

Voltage outputs from the thermocouples and the hot-wire sensors were recorded and amplified on the Beckman R511. The output of the Beckman recorder was also transmitted in individually shielded paired wires through a cable approximately 50 m long, to an Analogic AN 5800 analog to digital (A/D) Data Conversion System. Sample initialization and A/D conversion of the analog signals were controlled by programs of a PDP-11 computer. As the analog signals were digitized the digital signals were stored in the memory of the PDP-11 computer and then written on 9 track, 800 BPI magnetic tape. All operations were performed in real time. Subsequently, the magnetic tapes were converted, using a program written for the PDP-11 system, to 9-track, 800 BPI magnetic tapes compatible with the IBM 370/168.

In computing velocities, the hot wire calibration curves were fitted to fifth order polynomials. Velocities were then calculated assuming the normal cooling, cosine law.

The digital tapes were processed using a time series analysis program developed at the University of British Columbia, McBean [13], as adapted for use on the IBM 370/168 computer at Cornell University. The program which calculates variances,

covariances and spectral and cospectral densities uses an algorithm similar to the Fourier transform algorithm of Cooley and Tukey [14] for calculating transform coefficients. The variances and covariances presented are defined in terms of spectral and cospectral densities as:

$$\overline{u'^2} = \int_{f_1}^{f_2} \Phi_{u'}(f)\,\mathrm{d}f$$

$$\overline{v't'} = \int_{f_1}^{f_2} \Phi_{v't'}(f)\,\mathrm{d}f$$

$$\overline{u't'} = \int_{f_1}^{f_2} \Phi_{u't'}(f)\,\mathrm{d}f$$

where, for example, $\Phi_{u'}(f)$ is the contribution to the spectral density of $\overline{u'^2}$ in the frequency range f to $f + \mathrm{d}f$. The lower limit of integration f_1 is $1/T$ where T is the record length of the time series being analyzed. The upper integration limit f_2, the Nyquest frequency, is one-half the sampling rate.

The sampling rate used for the extraction of data was 50 samples/s, hence, $f_2 = 25$ Hz. The system for transmitting analog signals was checked by transmitting a sinusoidal signal generated by a Hewlett–Packard signal generator. A variance spectrum, calculated from a Fast–Fourier transform, indicated that the system of A/D Conversion did not introduce other peaks in the low frequency range.

A particular experiment was performed by traversing the boundary layer at a given downstream distance from the leading edge, x, for a given heat flux, q''. Heating times were limited to 25 min, after which a period of approximately 1 h was allowed for any disturbances and circulations to dampen. As necessary, the foil was subjected again to the same heat flux and measurements in the boundary layer were continued. The probe array could be positioned anywhere in the boundary region. The traversing mechanism employed allowed accurate displacements in the normal distance, y, and the vertical distance, x, as small as 0.0025 cm. The location of the surface was determined by the completion of a resistance circuit containing the foil itself and two stainless steel capillary tubes, adjacent to and parallel to the probe array. All experiments were carried out late at night to avoid the effects of large disturbances caused by the more intense daytime activity in the building. The mass and the capacity of the tank further cushioned it from disturbances.

3. EXPERIMENTAL RESULTS AND OBSERVATIONS

3.1. *Definition of transition events*

The results of Jaluria and Gebhart [2] showed conclusively that the beginning and end of transition are not correlated simply with the single parameter the Grashof number. In Fig. 1, the limits established by Jaluria and Gebhart [2] for the beginning of velocity and thermal transition and for the end of transition, are presented in terms of a modified Grashof number.

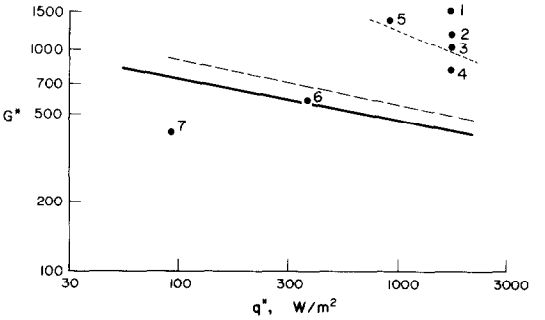

FIG. 1. Location of the beginning of velocity transition ——, thermal transition – – –, and the end of transition ....., from Jaluria and Gebhart [2]; points 1–7, conditions of present study.

$$G^* = 5 \cdot \left(\frac{g\beta x^4 q''}{5k\nu^2}\right)^{1/5},$$

where q'' is the surface heat flux. The points shown on this figure represent the particular experimental conditions of the present investigation. The experimental conditions corresponding to those points are shown in Table 1. The three lines correspond to the beginning of velocity transition (solid line), the beginning of thermal transition (dashed line), and the end of transition (dotted line). These three transition events were defined, respectively, as occurring with: (1) the observation of a jump in the velocity disturbance frequency above the filtered frequency; (2) the observation of a major distortion of the mean laminar temperature profile; and (3) the measured distributions, across the boundary layer, of velocity and temperature intermittancy, remaining unchanged downstream when the normal distance, y, is scaled with the measured local velocity and temperature boundary-layer thicknesses.

Table 1. Experimental conditions of the present study

Point No.	x(cm)	q''(W/m^2)	G^*
1	114.3	1920	1574
2	88.9	1920	1284
3	71.1	1920	1077
4	48.3	1920	787
5	114.3	1160	1419
6	48.3	436	587
7	48.3	95.3	440

The negative slopes of the transition lines indicate that the flow regimes are dependent upon both the Grashof number, G^*, and the heat flux, q''. For example, at $G^* = 700$ and $q'' = 60$ W/m^2 the beginning of transition has not yet occurred. However, at $G^* = 700$ and $q'' = 2000$ W/m^2, the flow is in transition. Note that along a vertical line of constant heat flux, q'', increasing Grashof numbers correspond to increasing distances downstream on a uniform flux plate.

3.2. *Growth of velocity and temperature fluctuation levels*

As the boundary layer underwent transition, Jaluria and Gebhart [2] reported that disturbances were amplified as they were convected downstream, although at decreasing rates. Temperature disturbances were reported to follow velocity disturbances and thermal transition did not occur until significant velocity fluctuations were present in the inner region of the boundary layer. Measurements of the amplification of maximum temperature fluctuation levels, $\overline{t'^2}$ and velocity fluctuation levels $\overline{u'^2}$, within the boundary layer, are presented in Fig. 2, in the later stages of transition. The plate heat flux, q'', was 1920 W/m^2 and the downstream location x varies from $x = 48.3$ to $x = 114.3$ cm, points 4, 3, 2, 1 in Fig. 1. For all locations, x, the maximum in the velocity fluctuation level occurred at approximately $\eta = 0.6$.

The maximum velocity fluctuation across the boundary layer achieves its highest magnitude around $x = 71.1$ cm (point 3 in Fig. 1) and then remains essentially constant. The maximum value is attained at approximately the location that Jaluria and Gebhart [2] designated as the end of transition, shown in Fig. 2.

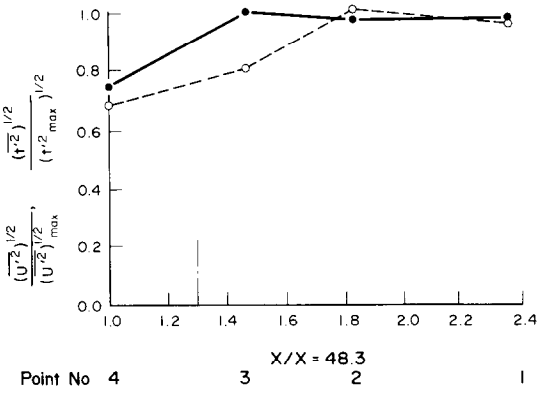

FIG. 2. Downstream growth of turbulent fluctuation levels $(\overline{u'^2})^{1/2}/[(\overline{u'^2})^{1/2}]_{max}$ ●, $(\overline{t'^2})^{1/2}/[(\overline{t'^2})^{1/2}]_{max}$ ○, vs $x/x = 48.3$ cm; $q'' = 1920$ W/m^2; vertical line is the end of transition determined by Jaluria and Gebhart [2].

The growth of temperature fluctuation lags behind the growth of velocity fluctuations, a continuation of the lag observed by Jaluria and Gebhart [2] in the early stages of transition. The maximum in temperature fluctuations is not attained until well beyond the end of transition. Heat-transfer results of Vliet and Liu [10] indicate that the region of fully developed turbulence, determined from heat transfer measurements, starts downstream of the location specified by Jaluria and Gebhart [2] as the end of transition. As points 1 and 2 in Fig. 1 lie within this region, it may be concluded that the turbulent heat-transfer mechanism is not fully developed until the maximum in temperature fluctuation level is reached, despite full development of both the intermittancy distribution and the velocity fluctuation level.

The lag between velocity and thermal transition mechanisms is a Prandtl number, Pr, effect. In water ($Pr \sim 6.0$), the thermal boundary layer is quite thin and the wall temperature gradient is steep. Viscous effects within the thermal boundary layer impede the penetration of turbulence from the outer boundary layer into the region of steep temperature gradients. Jaluria and Gebhart [2] observed a sharp drop in the local velocity and thermal intermittencies near the wall.

Increasing temperature fluctuation levels with increasing downstream location, x, followed by gradually decreasing fluctuation levels were reported by Papailou and Lykoudis [5] in a turbulent boundary layer in mercury. Grashof number levels were not reported and it may be inferred from the above discussion that the increasing temperature fluctuations were actually observed in transition.

3.3. *Profiles of temperature and velocity fluctuation levels*

In Fig. 3, the distributions of the temperature and velocity fluctuation levels across the boundary layer are presented, for the two most evolved turbulent flows studied here, points 1 and 2. The fluctuations are normalized by their respective maxima and plotted vs the similarity variable η. No sharp peak in the distribution is evidenced, in contrast to the results of Kutatelaze *et al.* [4]. A sharp peak would not be expected since turbulent diffusion would be expected to smooth out sharp gradients in the boundary layer.

The velocity fluctuation level determined here, by the RMS of the velocity fluctuation, are also quite different from the distribution presented by Jaluria and Gebhart [2], based entirely upon fluctuation maxima seen in an analog record. At the end of transition, Jaluria and Gebhart [2] report two peaks across the disturbance distribution, in η. The maximum occurs at $\eta = 2.8$. In light of the present results, as well as from other investigations, it seems plausible that these peaks represent the passage of particular bursts of turbulence. The observed unsystematic shift of the second peak to different locations in the boundary layer at different values of G^* in transition further assure that such peaks would not be statistically significant in an RMS representation.

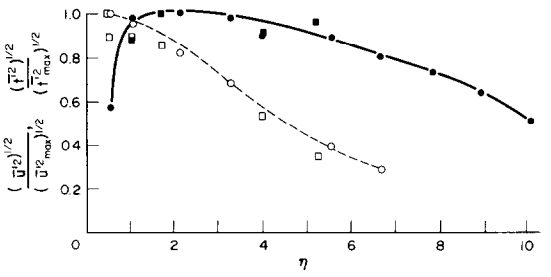

FIG. 3. Turbulent fluctuation levels across the boundary layer. $(\overline{u'^2})^{1/2}/[(\overline{u'^2})^{1/2}]_{max}$ ●, point 1, ■ point 2; $(\overline{t'^2})^{1/2}/[(\overline{t'^2})^{1/2}]_{max}$ vs η, ○ point 1, □ point 2.

The shape found, of the distribution of the temperature fluctuation, is similar to that reported by Papilou and Lykoudis [5] in mercury and Smith [9] in air. In mercury and air, the velocity and thermal boundary layers are about the same thickness. Therefore, layers of significant temperature and velocity fluctuations overlap. In water, the effect of the Prandtl number is to reduce the thickness of the temperature fluctuation layer in comparison to the layer with significant velocity fluctuations. In Fig. 3, the layer of large temperature fluctuation is approximately one-half the thickness of that of the velocity fluctuation.

3.4. *Turbulent intensities in transition*

A frequently quoted turbulence parameter in forced flow turbulence is intensity, i.e. $\overline{u'^2}/u_{max}$. It is plotted across the boundary region in Fig. 4,

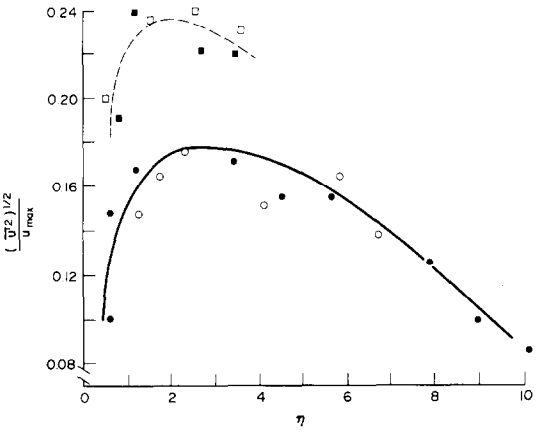

FIG. 4. Distributions of turbulent intensity across the boundary layer. ● point 1, ○ point 2, □ point 3, ■ point 5.

intensity normalized with the maximum local mean longitudinal velocity, u_{max}, for 4 different experimental conditions, points 1, 2, 3 and 5 in Fig. 1. For conditions corresponding to points 1 and 2, both for $q'' = 1920\,W/m^2$, the relative scale of turbulence is approximately the same. However, further upstream, point 3, the scale is greater. (Note the scale has been expanded to emphasize the difference in intensities.) The similarity of scales for points 1 and 2 suggests that the mechanisms for the creation of turbulent disturbances have been developed.

The intensity of turbulence in this natural convection flow is much greater than the turbulent intensity observed, for example, by Klebanoff [15] in a forced flow turbulent boundary layer in air on a flat plate at zero angle of incidence. The maximum intensity, observed near the surface of the plate, was 0.087. The intensity across the boundary layer decreased sharply from this maximum. In Fig. 4, intensities as high as about 0.18 may be observed for points 1 and 2 and to 0.24 for 3 and 5. The intensity remains high across much of the boundary layer. Thus, the longitudinal velocity fluctuations attained

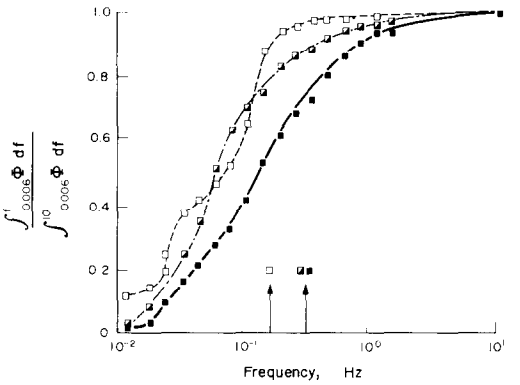

FIG. 5. Cumulative energy distribution vs frequency, at the beginning of transition, □ point 6, end of transition, □ point 3, in turbulence, ■ point 1.

for a given maximum velocity are much higher in the natural convection flow of this study than the comparable forced flow circumstance mentioned above.

As an indication of the dependence of transition on both G^* and q'', the turbulent intensity corresponding to point 5 is the same as that for point 3. The close proximity of points 3 and 5 to the end of transition line in Fig. 1 further strongly confirms the assertion of Jaluria and Gebhart [2] that flows along the locus of the end of transition line have reached the same state of transition.

3.5. *Temperature and velocity spectra*

After the initial onset of laminar instability, linear stability theory predicts, corroborated by measurement, that the spectrum of disturbance energy will come to be limited to a small band of frequencies. In transition, non-linear processes distort both the mean velocity and temperature profiles. However, much of the disturbance energy is still limited to a band of frequencies centered on the filtered frequency. Beyond transition, as turbulent kinetic energy is extracted from the mean flow through later non-linear processes, energy is distributed into disturbances over a much broader frequency range. A broad range of length scales or eddy sizes is expected to be characteristic of all turbulent flows as a result of the nonlinearity of the turbulent processes.

The observed filtered frequencies are extremely low. If disturbance frequency may be taken as a measure of turbulent length scales, then the length scales in transition would be large. Eventually, as energy is transferred from the highly amplified yet narrow band of frequencies centered on the filtered frequency, the large scale eddies should break down into smaller scales.

The substitution of frequency for wave-number is frequently justified by Taylor's hypothesis of "frozen turbulence". The applicability to shear flow of Taylor's hypothesis has been discussed extensively by Lumley [16]. Briefly, the validity of Taylor's hypothesis depends on the existence of a sufficiently small scale of turbulence $\overline{u'^2}/u_{max}$ and sufficiently

small velocity gradients, as compared to eddy sizes. Qualitatively, however, frequency and wave-number should be somewhat proportional. In Fig. 5, cumulative spectra, ($\int_{f_1}^{f} \Phi \, df$), for the disturbance energy, $\overline{u'^2}$, are presented for flows at the beginning of transition, the end of transition and in turbulence (points 6, 3 and 1 respectively in Fig. 3). Note points 3 and 1 are at the same heat flux at different downstream locations, x. The cumulative spectra takes into account only energy from 0.006 Hz to 10 Hz since above 10 Hz the low levels of the spectral density approached the noise levels of the anemometer unit. Arrows in Fig. 5, correspond to the filtered frequency predicted by linear stability theory.

Near the beginning of transition, point 6, approximately 45% of the disturbance energy is found in a small frequency range containing the predicted filtered frequency. Only 5% of the disturbance energy lies beyond the predicted filtered frequency. The unevenness of the cumulative frequency distribution at lower frequencies is attributable to changing patterns of flow (laminar to partially turbulent) occurring over relatively long periods of time, as well as to the development of large eddies.

At the end of transition, point 3, energy has been more evenly distributed across the spectrum. Approximately 14% of the energy is now distributed in the frequency range above the filtered frequency. This value is somewhat conservative, as the energy spectrum has been cut off at 10 Hz and some disturbance energy may be contained in the range above 10 Hz. Beyond the point designated as the end of transition by Jaluria and Gebhart [2] point 1, energy above the filtered frequency has increased but to only 27% of the total disturbance energy. Such an increase indicates the development of small scales within the boundary-layer structure.

As the spectrum of turbulence continues to develop, a condition may be reached in which regions of locally isotropic turbulence would exist at some length, the familiar "inertial subrange". Within inertial subrange, the spectral density of the kinetic energy of turbulence decays with wave number, k, as $k^{-5/3}$ (Obukhov [17]).

The assumptions of Obukhov [17] are concerned with the velocity spectra of incompressible flows. Corrsin [6] extended these ideas to include the spectra of temperature fluctuations, under conditions in which temperature could be considered to be a passive scalar in the flow field. This "convection subrange" also follows a "$-5/3$ law".

Two of the major assumptions in the identification of an inertial subrange are that the spectral density is a function only of the spectral density flux and wave number, and that the spectral density flux is constant. That is, within the inertial subrange, energy is not transferred into or out of the spectrum at particular wave numbers. The addition of buoyancy within a turbulent flow introduces the possibility that the spectral energy flux is not constant. Shur [7] presented spectra of velocities measured in clear air turbulence. The spectra decayed with wave number as k^{-3} at low wave numbers. At higher wave numbers, the "$-5/3$" subrange was observed. Lumley [8] asserted that an inertial subrange decaying as k^{-3}, followed by a $-5/3$ range results if the transfer of energy due to work done by buoyancy forces against gravity is small compared to the local spectral density flux.

Bolgiano [8], for flows with buoyancy, assumed a wave number range in which the spectrum is a function only of the net rate of dissipation of "mean-square fluctuations of buoyancy forces". This assumption leads to a $-11/5$ form for the velocity spectrum and a $-7/5$ form for the temperature spectrum.

Spectral densities, $\Phi(f)$ vs frequency, f, are presented in Fig. 6 for longitudinal velocity fluctuations and in Fig. 7 for temperature fluctuations at different locations across the boundary layer, for point 1. The spectra of velocity and temperature are quite similar. These spectra are very similar to the spectra associated with point 2. At low frequency there is large scatter between the spectra at different y locations. The spectrum exhibits many irregularities in the low frequency range, in contrast to the smooth spectrum exhibited at higher frequencies. The low frequency range corresponds to the large length scales at which energy is fed from the mean flow to the smaller turbulent eddies. The distribution of eddies, in the large scale range results from the

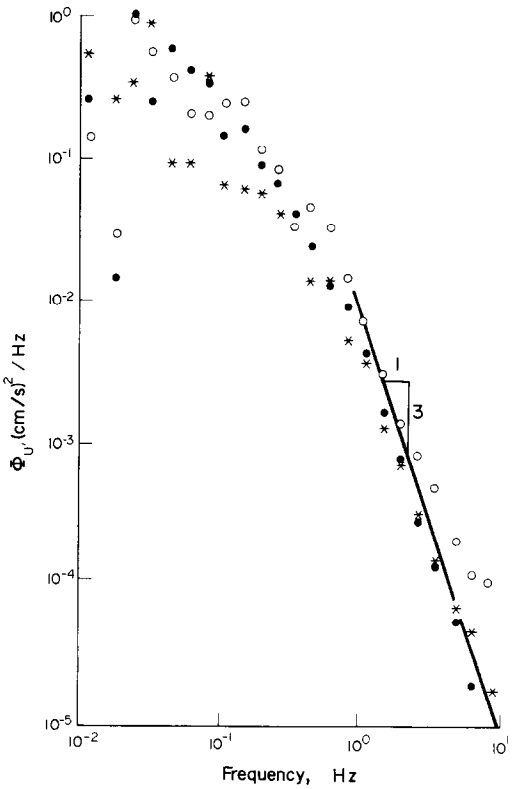

FIG. 6. Spectral density of velocity fluctuations, $\overline{u'^2}$, vs frequency for point 1, ● $\eta = 0.56$, ○ $\eta = 1.12$, ★ $\eta = 6.72$.

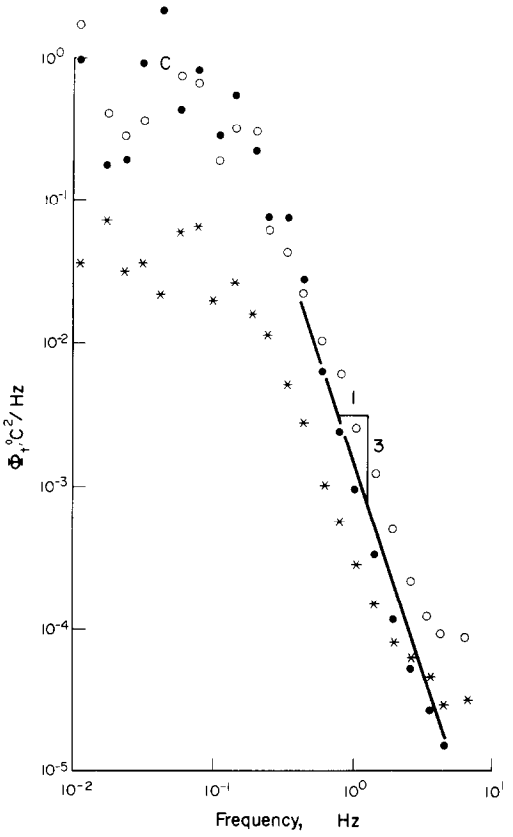

FIG. 7. Spectral density of temperature fluctuations, t'^2, vs frequency for point 1, ● $\eta = 0.56$, ○ $\eta = 1.12$, ★ $\eta = 6.72$.

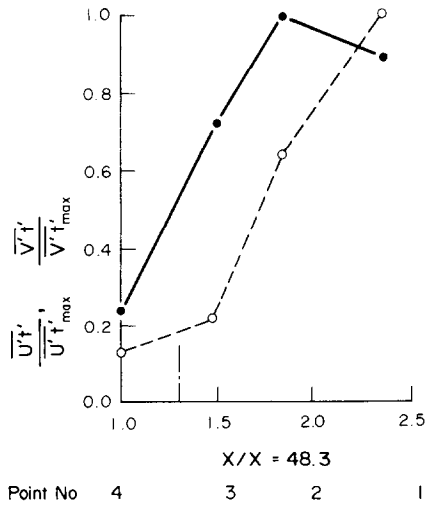

FIG. 8. Downstream growth of turbulent heat transport at $\eta \approx 0.6$, $\overline{u't'}/(\overline{u't'})_{max}$ ●, $\overline{v't'}/(\overline{v't'})_{max}$ ○ vs $x/x = 48.3$ cm; $q'' = 1920\,W/m^2$; vertical line is the end of transition from Jaluria and Gebhart [2].

limitations on scale imposed by the boundary-layer thickness. This scatter between the spectra suggests that the scale of large eddies varies across the boundary layer.

At higher frequencies, the velocity spectra at different y locations are reasonably similar, indicating the independence of small scales from the large scale eddies. Above 0.5 Hz, the decay in the spectra with frequency follows the "-3" law most closely.

At high frequencies, the temperature spectra also follow closely the "-3" law. The spectrum corresponding to the boundary-layer location, $\eta = 6.72$, is considerably displaced from the other two spectra. At this location the temperature fluctuation level, or frequency, is much lower.

Smith [9] reports temperature and longitudinal velocity spectra in air for an isothermal plate. Only a single point in transition is reported. However, for this point, a substantial region of both velocity and temperature spectra decay with wave number as k^{-3}. Thus, the spectra described above like those of Papailou and Lykoudis [5] and Smith [9] do suggest the validity of the assumption of Lumley [15]. That is, the extensive "-3" region indicates, that, locally, the spectral density may be considered to be constant and that an inertial subrange exists across a wide range of wave numbers.

3.6. *Turbulent heat transport*

Heat-transfer results (e.g. Cheesewright [19] and Vliet and Liu [10]) indicate that turbulent transport modes must develop to account for increased local heat transfer rates. Turbulent transport would be manifested though either turbulent convection of heat downstream $\rho C_p \overline{u't'}$ or through increased transport of heat from the inner wall region to the outer boundary layer, $\rho C_p \overline{v't'}$. In Fig. 8, the downstream development of these transport modes is shown for $q'' = 1920\,W/m^2$ at each of points 4, 3, 2, 1 in Fig. 1. At each x, the maximum of both $\overline{u't'}$ or $\overline{v't'}$, across the boundary layer, was found at approximately $\eta = 0.6$. Both modes of transport are seen to increase through the latter part of the transition regime, from 4 to 3, and in the completely turbulent regime. The maximum of both transport modes occurs beyond the location of the end of transition designated by Jaluria and Gebhart [2].

The downstream convection of heat is the sum of the convection by the mean base flow $\int_0^\infty \rho C_p u t \, dy$ and the turbulent downstream convection $\int_0^\infty \rho C_p \overline{u't'} \, dy$. As the boundary layer undergoes transition, the maximum of the mean longitudinal velocity falls from the laminar value [2]. For each of points 1, 2, 3, 4 in Fig. 1, the measured velocity maxima are approximately 50% of the calculated laminar maximum value. This decrease of the longitudinal velocity component, compared with the predicted laminar magnitude, occurs in the region of steep temperature gradients, near the wall. Hence, mean thermal transport is reduced. The turbulent transport mode $\rho C_p \overline{u't'}$ must account for this deficit.

Turbulent thermal transport normal to the surface is seen to increase, through, and well beyond the end of transition. The development of this mode, $\rho C_p \overline{v't'}$, is seen in Fig. 8 to lag the streamwise turbulent convective transport mode, $\rho C_p \overline{u't'}$ is coupled with

the decrease in the maximum of the mean longitudinal velocity profile as discussed above it would also be expected to be somewhat coupled to the growth of velocity fluctuations, u'^2.

A comparison of Fig. 8 and Fig. 2, which indicates the downstream growth of velocity fluctuations, $\overline{u'^2}$, and temperature fluctuation, $\overline{t'^2}$, suggests that the development of the normal heat-transport mode is more closely coupled to the growth of high temperature fluctuation levels in the wall region. The sharp rise in both transport modes beyond the end of transition is expected since the heat-transfer results of Vliet and Liu [10] indicate that a fully developed heat-transfer mechanism is not attained until beyond the end of transition designated by Jaluria and Gebhart [2].

The profile across the boundary layer, of transport modes $\rho C_p \overline{u't'}$ and $\rho C_p \overline{v't'}$, are presented in normalized form in Fig. 9(a) and (b) at point 1. Each is normalized with its maximum value found across the boundary layer. The correlation coefficients

$$R_{u't'} = \frac{\overline{u't'}}{(\overline{u'^2})^{1/2}(\overline{t'^2})^{1/2}}$$

$$R_{v't'} = \frac{\overline{v't'}}{(\overline{v'^2})^{1/2}(\overline{t'^2})^{1/2}}$$

are also shown. Both $\overline{u't'}$ and $\overline{v't'}$ are maximum close to the wall and decrease through the boundary layer. The correlation coefficients, which may be thought of as measures of transport efficiency, are also maximum near the wall and decrease through the boundary layer. The velocity and temperature disturbances, u' and t', are most strongly correlated near the wall. However, v' and t' in Fig. 9(b) are essentially uncorrelated throughout the boundary layer. Perhaps at locations closer to the wall, that is, within the region of higher temperature gradients, v' and t' would be more strongly correlated. The strong correlation associated with covariance $\overline{u't'}$ results from the coupling of the temperature field to the longitudinal velocity field through buoyancy. Large temperature fluctuations of large scale give rise to buoyancy concentration, which cause large longitudinal velocity fluctuations.

3.7. *Comparisons of reported transition events*

In Table 2, transition events are tabulated in terms of G^* for approximately a given level of heat flux

Table 2. Comparison of reported transition events as a function of G^* for $q'' \simeq 1920\ \mathrm{W/m^2}$

	G^*	$q''(\mathrm{W/m^2})$
End of transition [Jaluria and Gebhart (2)]	1000	1920
Developed turbulence [Vliet and Liu (10)]	1245	1970
Point 2 – region of spectral transition	1284	1920

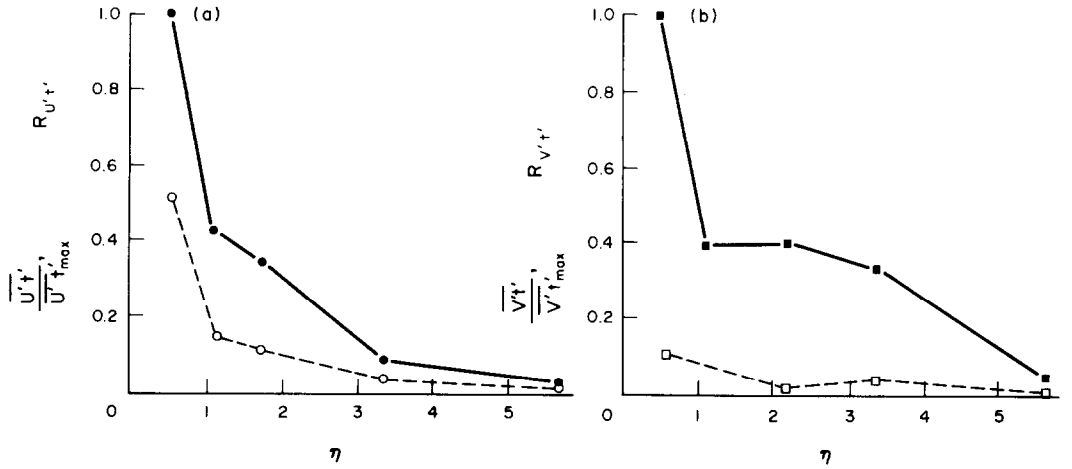

FIG. 9. Distributions of normalized heat transport and correlation coefficient across the boundary layer for point 1. (a) ● $\overline{u't'}/(\overline{u't'})_{max}$, ○ $R_{u't'}$ vs η, (b) ■ $\overline{v't'}/(\overline{v't'})_{max}$, □ $R_{v't'}$ vs η.

from the results of Jaluria and Gebhart [2], Vliet and Liu [10] and the present study. Jaluria and Gebhart [2] established the relationship between G^* and q'' for which the intermittency distributions across the boundary layer of temperature and velocity have stabilized. Figures 3 and 5 indicate that at the end of transition the level of velocity fluctuation $\overline{u'^2}$, has also stabilized. However, the results of this investigation indicate that the lag in thermal transition reported by Jaluria and Gebhart [2] in the early stages of transition is still in evidence in the growth lag of temperature fluctuation level, $\overline{t'^2}$, (Fig. 2) and both turbulent transport modes (Fig. 8).

Vliet and Liu [10] measured the local heat-transfer coefficient, h, for a constant flux plate in water. A transition regime for this parameter was observed in which h deviating from the predictions of laminar boundary-layer theory, abruptly increased with downstream location x. Then h gradually decreased with x. In Table 2, we have designated the point at

which the local transfer coefficient begins to decrease as developed turbulent flow.

Point 2 in Figs. 2 and 8 corresponds to the condition for which the maximum values of the temperature fluctuation level, $\overline{t'^2}$, and the transport mechanism, $\rho C_p \overline{u't'}$, were measured. As discussed above the development of these parameters occurs within a regime of spectral transition. Thus, the data of Vliet and Liu [10] indicates that a fully developed turbulent heat-transfer mechanism is not evolved until the energy spectrum and transport modes are fully developed.

4. CONCLUSIONS

The development of a vertical natural convection boundary layer from transition to turbulence involves the simultaneous development of several dependent transport parameters. First the intensity of turbulence grows as large eddies develop disrupting the organized laminar flow. In water, where the Prandtl number is greater than one, velocity transition begins first. The intensity of turbulent temperature fluctuations then follows the growth of velocity disturbance field and thermal transition occurs. With the final vanishing of the laminar flow field, the transition regimes come to an end. However, beyond the end of transition, a regime of spectral and transport development occurs. The disturbance field, first dominated by a filtering mechanism expands to include a spectrum of turbulent eddies. Spectral measurements indicate that the turbulent eddies, over a wide range of wave-numbers, are strongly affected by buoyant-production of turbulence. Although the growth of velocity disturbances has levelled out by the end of the transition, the temperature disturbance levels continue to grow and turbulent transport accounts for an increasing proportion of heat transport.

Acknowledgements—The authors wish to acknowledge the support of the National Science Foundation under grants GK18529, ENG75-01466, ENG75-22623, and the support of the U.S. Dept. of Interior, Office of Water Research and Technology.

REFERENCES

1. B. Gebhart, Instability, transition, and turbulence in buoyancy-induced flows, *Ann. Rev. Fluid Mech.* **5**, 213 (1973).
2. Y. Jaluria and B. Gebhart, On transition mechanisms in vertical and natural convection flow, *J. Fluid Mech.* **66**, 709 (1974).
3. F. Godaux and B. Gebhart, An experimental study of the transition of natural convection flow adjacent to a vertical surface, *Int. J. Heat Mass Transfer* **17**, 93 (1974).
4. S. S. Kutztelaze, A. G. Kirdyashkin and V. P. Ivakin, Turbulent free convection on a vertical plate and in a vertical layer, *Int. J. Heat Mass Transfer* **15**, 193 (1972).
5. D. D. Papailou and P. S. Lykoudis, Turbulent free convection flow, *Int. J. Heat Mass Transfer* **17**, 161 (1974).
6. S. Corrsin, On the spectrum of isotropic temperature fluctuations in an isotropic turbulence, *J. Appl. Phys.* **22**, 469 (1951).
7. G. N. Shur, Eksperimental 'nyye issledovaniya energeticheskogo spectra atmosfernoy turbulentnost, *Trudy* **43**, 79, Trans. as AID Report T-63-55 Aerospace Info. Div. Lib. Cong. (1962).
8. J. L. Lumley, The spectrum of nearly inertial turbulence in a stably stratified fluid, *J. Atmos. Sci.* **21**, 99 (1964).
9. R. R. Smith, Characteristics of turbulence in free convection flow past a vertical plate, Ph.D. Thesis, University of London, Queen Mary College (1972).
10. G. C. Vliet and C. K. Liu, An experimental study of turbulent natural convection boundary layers, *J. Heat Transfer* **91**, 517 (1969).
11. K. Hollasch, A survey of the literature, design, and experimental verification of a measurement scheme for external turbulent natural convection flow, M.S. Thesis, Cornell University (1970).
12. K. Hollasch and B. Gebhart, Calibration of constant temperature hot-wire anemometers at low velocities in water with variable fluid temperature, *J. Heat Transfer* **94**, 17 (1972).
13. G. A. McBean, The turbulent transfer mechanisms in the atmospheric surface layer, Ph.D. Thesis, University of British Columbia (1968).
14. J. W. Cooley and O. W. Tukey, An algorithm for the machine calculation of complex Fourier series, *Math. Comp.* **19**, 297 (1965).
15. P. S. Klebanoff, Characteristics of turbulence in a boundary layer with zero pressure gradient, NACA TN-3178 (1954).
16. J. L. Lumley, On the interpretation of time spectra measured in high intensity shear flows, *J. Atmos. Sci.* **21**, 99 (1965).
17. A. M. Obukhov, Energy distribution in the spectrum of a turbulent flow, *Izv. Akad. Nauk. SSSR, Ser. Geog., Geofiz.* **4–5**, 453 (1941).
18. R. Bolgiano, Structure of turbulence in a stratified media, *J. Geophys. Res.* **64**, 2226 (1962).
19. R. Cheesewright, Turbulent natural convection from a vertical plane surface, *J. Heat Transfer* **90**, 1 (1968).

DEVELOPPEMENT DU TRANSPORT TURBULENT DANS UNE COUCHE LIMITE DE CONVECTION NATURELLE VERTICALE

Résumé Trois sondes calibrées à fil chaud et un thermocouple permettent la mesure des composantes longitudinale et normale de vitesse u et v, et de la température t, dans l'écoulement de transition d'une couche limite de convection naturelle adjacente à une surface verticale avec flux thermique constant. Les signaux analogiques de la sonde sont digitalisés et enregistrés sur bande magnétique en temps réel. Les données digitales sont traitées en utilisant l'algorithme de transformée rapide de Fourier pour calculer les variances $\overline{u'^2}$, $\overline{t'^2}$, les covariances $\overline{u'v'}$, $\overline{v't'}$, les coefficients de corrélation $\overline{R_{v't'}}$, $\overline{R_{u't'}}$, les spectres de $\overline{u'^2}$ et $\overline{t'^2}$. Dans la transition, les niveaux de fluctuation de vitesse et de température $\overline{u'^2}$ et $\overline{t'^2}$ croissent avec la distance en aval et le spectre de perturbation s'élargit en domaine de fréquence. A la fin de la transition, la croissance des fluctuations de vitesse $\overline{u'^2}$ est fortement réduite. Un autre régime d'écoulement dans la transition a été identifié dans lequel le spectre des fluctuations de vitesse continue à s'élargir et les niveaux de fluctuations de température $\overline{t'^2}$ aussi bien que les flux thermiques turbulents continuent à croître.

DIE ENTWICKLUNG VON TURBULENTEM TRANSPORT IN EINER VERTIKALEN GRENZSCHICHT BEI FREIER KONVEKTION

Zusammenfassung Drei kalibrierte Hitzdrahtfühler und ein Thermoelement wurden benutzt, um die Längs- und Querkomponenten u und v der Geschwindigkeit und die Temperatur t im Übergangsgebiet der Strömung in einer durch Auftrieb erzeugten Grenzschicht nahe einer vertikalen Wand mit konstanter Wärmestromdichte zu messen. Die Analogsignale des Fühlers wurden digitalisiert und in Echtzeit auf Magnetband aufgezeichnet. Die Digitalwerte wurden unter Verwendung eines Algorithmus für schnelle Fourier Transformation verarbeitet, um Varianzen $\overline{u'^2}$ und $\overline{t'^2}$, Kovarianzen $\overline{u'v'}$ und $\overline{v't'}$, Korrelationskoeffizienten $R_{v't'}$, $R_{u't'}$; sowie die Varianzspektren von $\overline{u'^2}$ und $\overline{t'^2}$ zu berechnen. Beim Übergang nahmen die Fluktuationsgrade $\overline{u'^2}$ und $\overline{t'^2}$ der Geschwindigkeiten und Temperaturen mit zunehmendem Abstand stromabwärts zu, und das Spektrum der Störungen verbreiterte sich zu einem größeren Frequenzbereich. Am Ende des Übergangs war der Zuwachs der Geschwindigkeitsfluktuationen $\overline{u'^2}$ deutlich herabgesetzt. Jedoch wurde jenseits des Übergangsgebiets ein weiteres Strömungsgebiet identifiziert, in welchem die Spektren der Geschwindigkeitsfluktuationen sich weiter verbreiterten und die Fluktuationsgrade $\overline{t'^2}$ der Temperatur wie auch die turbulenten Wärmeströme weiter zunahmen.

РАЗВИТИЕ ТУРБУЛЕНТНОГО ПЕРЕНОСА В ВЕРТИКАЛЬНОМ СВОБОДНОКОНВЕКТИВНОМ СЛОЕ

Аннотация — С помощью трёх калиброванных термоанемометров и термопары проводились измерения продольной и нормальной компонент скорости, u и v, а также температуры, t, при нестационарном режиме течения в свободноконвективном восходящем пограничном слое у вертикальной поверхности с постоянным подводом тепла. Аналоговые сигналы термоанемометра преобразовывались в цифровую форму и записывались на магнитную ленту в реальном масштабе времени. Цифровые данные обрабатывались с помощью алгоритма быстрого преобразования Фурье, для того чтобы можно было рассчитать дисперсии $\overline{u'^2}$, $\overline{t'^2}$, функции корреляций $\overline{u'v'}$, $\overline{v't'}$, коэффициенты корреляций $R_{v't'}$, $R_{u't'}$ и спектры дисперсии $\overline{u'^2}$ и $\overline{t'^2}$. В переходном режиме уровни флуктуаций скорости и температуры, $\overline{u'^2}$ и $\overline{t'^2}$, возрастали с ростом расстояния вниз по течению, а спектр возмущений охватывал более широкий диапазон частот. В конце переходного режима рост флуктуаций скорости, $\overline{u'^2}$, резко замедлялся, и за областью перехода возникал другой режим течения, в котором спектры флуктуаций скорости продолжали расширяться, а степень флуктуаций температуры, $\overline{t'^2}$, как и величина турбулентного теплового потока, продолжали возрастать.